

Multiparameter approach to quantum phase estimation with limited visibility: supplementary material

EMANUELE ROCCIA¹, VALERIA CIMINI¹, MARCO SBROSCIA^{1,*}, ILARIA GIANANI¹, LUDOVICA RUGGIERO¹, LUCA MANCINO¹, MARCO G. GENONI², MARIA ANTONIETTA RICCI¹, AND MARCO BARBIERI¹

¹Dipartimento di Scienze, Università degli Studi Roma Tre, Via della Vasca Navale 84, 00146, Rome, Italy

²Quantum Technology Lab, Dipartimento di Fisica, Università degli Studi di Milano, 20133, Milan, Italy

*Corresponding author: marco.sbroscia@uniroma3.it

Published 24 September 2018

This document provides supplementary information to "Multiparameter approach to quantum phase estimation with limited visibility" <https://doi.org/10.1364/optica.5.001171>. Here we detail the calculations used in the main text.

1. EVOLUTION OF THE TWO-PHOTON STATE UNDER PHASE ROTATION

The aim of this section is to obtain detection the probabilities from a two-photon $N00N$ state with limited visibility, following a phase shift ϕ . We start by noticing that the combination of a beam splitter (BS), a phase shift ϕ , and a second BS can be modelled as an unbalanced BS with transmission $\cos(\phi/2)$. Since we use the polarization degree of freedom of a single spatial mode, the phase shift can be implemented as a polarization rotation by means of a half wave plate, as in the calibration phase, or of an optically active solution. The mode mixing performs the transformation:

$$\begin{aligned} a_H &\rightarrow \cos(\phi/2)a_H + \sin(\phi/2)a_V \\ a_V &\rightarrow \cos(\phi/2)a_V - \sin(\phi/2)a_H \end{aligned} \quad (S1)$$

The first step considers perfectly indistinguishable photons in the two-photon state $|\Psi_0\rangle_{in} = \hat{a}_H^\dagger \hat{a}_V^\dagger |0\rangle$, which evolve following the phase shift:

$$\begin{aligned} |\Psi_\phi\rangle_{in} &= \left[\cos\left(\frac{\phi}{2}\right) \hat{a}_H^\dagger + \sin\left(\frac{\phi}{2}\right) \hat{a}_V^\dagger \right] \left[\cos\left(\frac{\phi}{2}\right) \hat{a}_V^\dagger - \sin\left(\frac{\phi}{2}\right) \hat{a}_H^\dagger \right] |0\rangle \\ &= \left[\cos(\phi) \hat{a}_H^\dagger \hat{a}_V^\dagger - \sin(\phi) \frac{(\hat{a}_H^{\dagger 2} - \hat{a}_V^{\dagger 2})}{2} \right] |0\rangle. \end{aligned} \quad (S2)$$

A half wave plate (HWP) is inserted, and set at an angle θ with respect to the horizontal; its effect on the two-photon state delivers the expression

$$|\Psi_{\phi;\theta}\rangle_{in} = \cos(\phi) \left[-\cos(4\theta) \hat{a}_H^\dagger \hat{a}_V^\dagger + \frac{1}{2} \sin(4\theta) (\hat{a}_H^{\dagger 2} - \hat{a}_V^{\dagger 2}) \right] |0\rangle - \sin(\phi) \left[\sin(4\theta) \hat{a}_H^\dagger \hat{a}_V^\dagger + \frac{1}{2} \cos(4\theta) (\hat{a}_H^{\dagger 2} - \hat{a}_V^{\dagger 2}) \right] |0\rangle, \quad (S3)$$

from which the following probabilities can be obtained:

$$\begin{aligned} p_{in}(1|\theta; \phi) &= \frac{1}{2} (1 + \cos(8\theta - 2\phi)) \\ p_{in}(2|\theta; \phi) &= \frac{1}{2} \sin^2(4\theta - \phi). \end{aligned} \quad (S4)$$

Using the same approach, it is possible to calculate the evolution of quantum state $|\Psi_0\rangle_{dis} = \hat{a}_H^\dagger \hat{b}_V^\dagger |0\rangle$ for two distinguishable photons: here we also need considering two extra modes a_V and b_H , initially in the vacuum mode, to define transformations similar to

the ones in Eq. (S1). These then give an expression for the state as:

$$\begin{aligned} |\Psi_\phi\rangle_{dis} &= \left[\cos\left(\frac{\phi}{2}\right) \hat{a}_H^\dagger + \sin\left(\frac{\phi}{2}\right) \hat{a}_V^\dagger \right] \left[\cos\left(\frac{\phi}{2}\right) \hat{b}_V^\dagger - \sin\left(\frac{\phi}{2}\right) \hat{b}_H^\dagger \right] |0\rangle \\ &= \left[\cos\left(\frac{\phi}{2}\right)^2 \hat{a}_H^\dagger \hat{b}_V^\dagger - \sin\left(\frac{\phi}{2}\right)^2 \hat{a}_V^\dagger \hat{b}_H^\dagger - \sin(\phi) \frac{(\hat{a}_H^\dagger \hat{b}_H^\dagger - \hat{a}_V^\dagger \hat{b}_V^\dagger)}{2} \right] |0\rangle. \end{aligned} \quad (S5)$$

and then, including the HWP, the probabilities:

$$\begin{aligned} p_{dis}(1|\theta; \phi) &= \frac{1}{4}(3 + \cos(8\theta - 2\phi)) \\ p_{dis}(2|\theta; \phi) &= \frac{1}{4}\sin^2(4\theta - \phi). \end{aligned} \quad (S6)$$

These have been obtained considering detectors unable to distinguish between the modes a and b .

In the general case, the initial mode b_V will possess a component a_V indistinguishable from a_H in all other degrees of freedom, and a distinguishable component q_V : $b_V^\dagger = \sqrt{1 - \epsilon^2} a_V^\dagger + \epsilon q_V^\dagger$. As before, we need to introduce extra vacuum modes. The final probabilities will be given by the weighted sums:

$$\begin{aligned} p(1|\theta; \phi, \epsilon) &= (1 - \epsilon^2) p_{in}(1|\theta; \phi) + \epsilon^2 p_{dis}(1|\theta; \phi) = \frac{1 - \epsilon^2}{2} (1 + \cos(8\theta - 2\phi)) + \frac{\epsilon^2}{4} (3 + \cos(8\theta - 2\phi)) \\ p(2|\theta; \phi, \epsilon) &= (1 - \epsilon^2) p_{in}(2|\theta; \phi) + \epsilon^2 p_{dis}(2|\theta; \phi) = \frac{1 - \epsilon^2}{2} \sin^2(4\theta - \phi) + \frac{\epsilon^2}{4} \sin^2(4\theta - \phi). \end{aligned} \quad (S7)$$

These expressions can be cast in more compact form by introducing the visibility v of the predicted fringes as $v = (2 - \epsilon^2)/(2 + \epsilon^2)$:

$$\begin{aligned} p(1|\theta; \phi, v) &= \frac{1}{1 + v} (1 + v \cos(8\theta - 2\phi)) \\ p(2|\theta; \phi, v) &= \frac{v}{1 + v} \sin^2(4\theta - \phi). \end{aligned} \quad (S8)$$

2. OPTIMAL MEASUREMENT FOR SINGLE PARAMETER ESTIMATION APPROACH

We now investigate the performance of phase estimation using a single-parameter approach that relies on a pre-calibration of the visibility v_0 . The post-selected probabilities are given by

$$p(\theta|\phi) = \frac{1}{4}(1 + v_0 \cos(8\theta - 2\phi)), \quad (S9)$$

where the error on v_0 is considered negligible.

The ultimate bound on the phase precision is than given by $1/M\mathcal{F}_{\phi\phi}$: we compare the uncertainties on the phase to this limit, considering three instances for the visibility, namely the maximum, the mean and the minimum values obtained in the multiparameter analysis. By inspecting Fig. S1 it is revealed how the extreme values v_{min} or v_{max} may lead to an estimation with subtle departures from the corresponding CRBs. The use of the mean visibility mitigates such discrepancies, although it manifests differences with respect to the CRB three times larger than those achieved with the multi-parameter approach. Even in such controlled conditions some effect of the bias on the uncertainties can be assessed.

The effect can be made more evident when exploring the sucrose solution with a single-parameter approach. Fig S2 shows what happens when v_0 is not properly considered: the presence of the sample has reduced it with respect to the value registered at the test stage. The effect of bias is limited only around the measured value of v_0 ; we quantify this by the quantity $K_M = \sigma^2 \mathcal{F}_{\phi, \phi} M$. This quantity, calculated for the variance on ϕ from the multiparameter approach, shows that part of the resources needed to be devoted to visibility estimation: this does not fall on the single-parameter CRB despite being compatible with that of the multiparameter approach.

3. EFFECTS OF THE POST-SELECTION ON THE FISHER INFORMATION

The set Eq. (S8) describe the probabilities of a three-outcome POVM for any given θ . We can generalise this to a set of $m \times 3$ outcomes by choosing m different values of θ with different probabilities $p(\theta)$; the relevant case for our experiment has $m = 4$ with $\theta = \{0, \pi/16, \pi/8, 3\pi/16\}$, and a flat distribution for the settings $p(\theta) = 1/4$. The Fisher information matrix associated to this strategy is found as:

$$F_{ij} = \frac{1}{4} \sum_{\theta} \left(\frac{\partial_i p(1|\theta; \phi, v) \partial_j p(1|\theta; \phi, v)}{p(1|\theta; \phi, v)} + 2 \frac{\partial_i p(2|\theta; \phi, v) \partial_j p(2|\theta; \phi, v)}{p(2|\theta; \phi, v)} \right), \quad (S10)$$

for $i = \phi, v$ and likewise for j . We remark that with photon number resolving detectors, a POVM with $m = 2$ settings would be able to provide the same Fisher information.

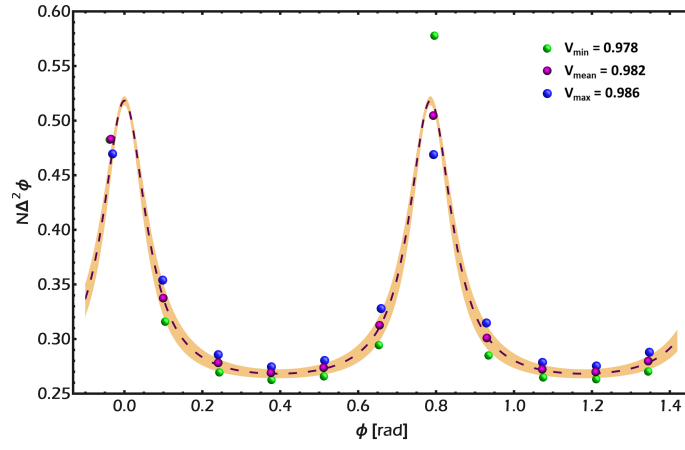


Fig. S1. The estimated phase variance for three values of visibility, $v_{\min} = 0.978$ (green dots), $v_{\text{mean}} = 0.982$ (purple dots), $v_{\max} = 0.986$ (blue dots), compared with the expected CRB for pre-calibrated visibilities ranging from $v_0 = v_{\min}$ to $v_0 = v_{\max}$ (shaded area): $v_0 = v_{\text{mean}}$ is highlighted (purple dashed line).

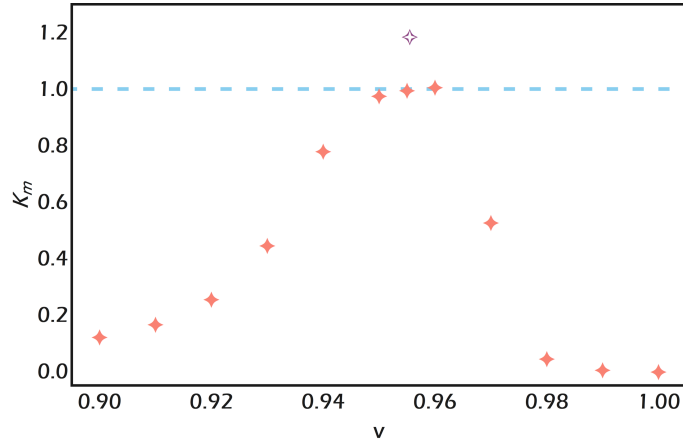


Fig. S2. The estimated phase variance in units of $1/(M\mathcal{F}_{\phi,\phi})$ for the sucrose solution as a function of the pre-set visibility v . The solid diamonds refer to the single-parameter strategy, while the open diamond is for the variance derived from the multiparameter.

In the actual experiment, we have no access to the full set of the outcomes, since we did not use photon number resolving detectors. We then use the post-selected probabilities

$$p(\theta|\phi, v) = \frac{1}{4} (1 + v \cos(8\theta - 2\phi)) \quad (\text{S11})$$

associated to coincidence counts only, and obtained by normalising each of the four $p_1(\theta|\phi, v)$ to their sum. As described in the main text, in the post-selected picture, the setting θ plays the role of the measurement outcome: given the coincidence event Eq. (S11) quantifies the probability that this has occurred by setting the HWP angle at the value θ . The post-selected Fisher information is then given by:

$$F_{ij}^{PS} = \frac{1}{4} \sum_{\theta} \frac{\partial_i p(\theta|\phi, v) \partial_j p(\theta|\phi, v)}{p(\theta|\phi, v; \theta)}, \quad (\text{S12})$$

which is the one used in the main text. The explicit forms are:

$$\mathcal{F}_{\phi,\phi} = 4 - \frac{16(v^4 - 3v^2 + 2)}{(1 - \cos(8\phi))v^4 - 8v^2 + 8} \quad (\text{S13})$$

$$\mathcal{F}_{\phi,v} = -\frac{2v^3 \sin(8\phi)}{(1 - \cos(8\phi))v^4 - 8v^2 + 8} \quad (\text{S14})$$

$$\mathcal{F}_{v,v} = \frac{4 - (1 - \cos(8\phi))v^2}{(1 - \cos(8\phi))v^4 - 8v^2 + 8}. \quad (\text{S15})$$

We notice that adopting this strategy results in a loss of the useful resources by a factor 2.

A comparison of the two Fisher matrices is carried out in Fig. S3: post-selection affects phase estimation by reducing the available information $F_{\phi,\phi}$, while the visibility estimation appears improved by a higher value of $F_{v,v}$. We notice that this increase, however, does not compensate the loss of resources: if one takes into account the probability of the favourable events that are post-selected, the weighted post-selected Fisher Information is in general always lower than the Fisher information of the complete POVM. Furthermore, the correlation properties are also made tighter: this is verified by introducing a normalised value for the off-diagonal terms as $\zeta_{\phi,v} = F_{\phi,v}/(F_{\phi,\phi}F_{v,v})^{1/2}$ showing more pronounced oscillations. Notice that no spurious correlations are introduced when these are absent in the original POVM.

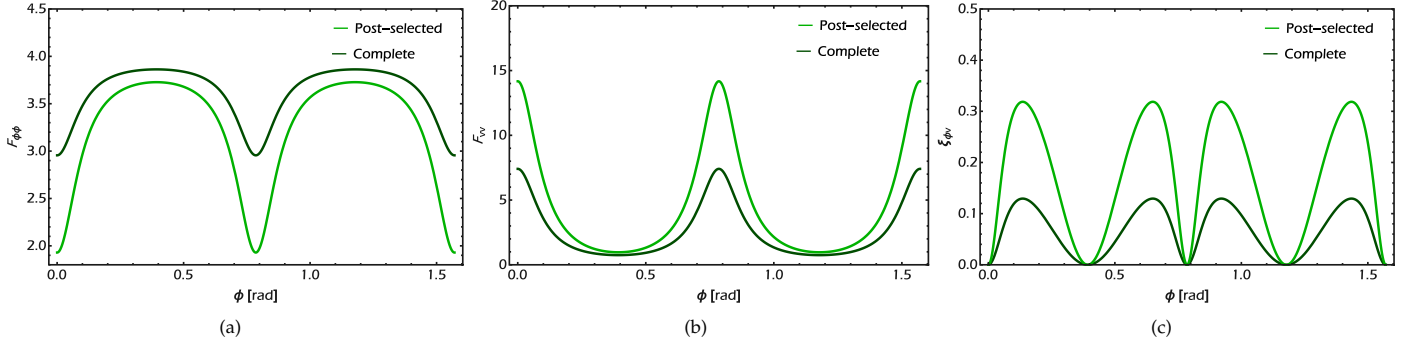


Fig. S3. The post selected (bright green line) and complete (dark green line) Fisher information matrix elements, $F_{\phi,\phi}$ (a), $F_{v,v}$ (b) and $\zeta_{\phi,v}$ (c).

4. HYPOTHESIS TEST FOR THE COVARIANCE MATRICES.

To put on a quantitative ground how close the experimental joint density distribution is to the one expected at the CRB, we test the null hypothesis $H_0 : \Sigma = \mathcal{F}^{-1}/M$. The test statistics we used is the likelihood ratio l reported in Eq.9 of the main text. Under H_0 such a variable is distributed as a chi-squared variable with 3 degrees of freedom, χ_3^2 . We fixed the confidence level at $1 - \alpha = 0.95$ as customary, which fixes the critical value, l_c , at which $P(l > l_c) = \alpha = 0.05$ to $l_c = 7.81$. Since for both the two sugary solutions we have considered the retrieved l value is lower than l_c , with can affirm at 0.05 significance level that the experimental coherence matrix is compatible with the one at the CRB.

5. GENERALIZATION TO 2N-PHOTON HOLLAND BURNETT STATES

We now generalize our approach to arbitrary Holland-Burnett states, obtained by the interference of two N -photon Fock states. The initial state is

$$|\Psi_0\rangle = \frac{1}{N!} (a_H^\dagger)^N (b_V^\dagger)^N |0\rangle = \frac{1}{N!} (a_H^\dagger)^N (q_H^\dagger)^0 \sum_{k=0}^N \binom{N}{k} (1 - \epsilon^2)^{k/2} \epsilon^{(N-k)/2} (a_V^\dagger)^k (a_V^\dagger)^{N-k} |0\rangle. \quad (\text{S16})$$

Here we have operated the same modal decomposition as before to introduce distinguishability, and we have made the presence of the extra modes explicit. If the transformations Eq. (S1) are imposed on the pairs of modes a_H and a_V , and q_H and q_V , the evolved state $|\Psi_\phi\rangle$ can be calculated. In the general case, an additional controlled phase θ can be introduced, which corresponds to different measurement settings.

The POVM we consider counts the total photon number on modes a_H and q_H , without resolving the individual populations; due to photon number correlations, adding a second counter on the modes a_V and q_V would provide no extra information. The operator associated to the outcome x is then written in the Fock basis as:

$$\Pi_x = \sum_{s=0}^x \Pi_x^{(s)} = \sum_{s=0}^x |s\rangle\langle s|_{a_H} \otimes I_{a_V} \otimes |x-s\rangle\langle x-s|_{q_H} \otimes I_{q_V}. \quad (\text{S17})$$

Each detection probability is then found as $p(x, \theta | \phi, \epsilon) = \langle \Psi_{\phi+\theta} | \Pi_x | \Psi_{\phi+\theta} \rangle = \sum_{s=0}^x p^{(s)}(x, \theta | \phi, \epsilon)$ for all possible outcomes $x = 0, \dots, 2N$. In our calculations we considered two possible settings $\theta = 0$ and $\theta = \pi/2$, alternated with equal probability.